

Suppression of magnetism in $\text{SrFe}_{2-x}\text{Ru}_x\text{As}_2$: First-principles calculations

Guangtao Wang, Lihua Zheng, Minping Zhang, and Zongxian Yang

College of Physics and Information Engineering, Henan Normal University, Xinxiang, Henan 453007, People's Republic of China

(Received 5 October 2009; revised manuscript received 23 December 2009; published 22 January 2010)

The magnetism in SrFe_2As_2 can be suppressed by electron doping with a small substitution of Fe by Co or Ni, giving the way to superconductivity. Using the virtual-crystal approximation, we find the isoelectronic substitution of Fe with Ru suppresses the spin-density-wave characteristic of SrFe_2As_2 by decreasing the Stoner enhancement and increasing the bandwidth due to the more extended bandwidth of Ru $4d$ compared with that of Fe $3d$. Although Ru is isoelectronic with Fe, such substitution changes the Fermi surface and band structure greatly. From the first-principles calculation, we find the phase diagram of $\text{SrFe}_{2-x}\text{Ru}_x\text{As}_2$ can be sorted as three different phases: (I) the stripe antiferromagnetic state ($0.0 \leq x < 0.6$); (II) the low spin state ($0.6 \leq x < 1.0$), and (III) the nonmagnetic state ($1.0 \leq x \leq 2.0$). In phase II, the spin-density wave is suppressed greatly, accompanying with the emergence of superconductivity.

DOI: [10.1103/PhysRevB.81.014521](https://doi.org/10.1103/PhysRevB.81.014521)

PACS number(s): 74.25.Ha, 71.18.+y, 71.20.-b

I. INTRODUCTION

The recent discovery¹ of superconductivity in the FeAs-based compound $\text{LaFeAsO}_{1-x}\text{F}_x$ with transition temperature $T_C=26$ K has generated great excitement. Subsequently, other related compounds $\text{LnFeAsO}_{1-x}\text{F}_x$ ($\text{Ln}=\text{Sm}, \text{Nd}$, and Ce) have been synthesized with T_C ranging from 10 K to as high as 55 K.²⁻⁵ Later, three new series of compounds $\text{A}_{1-x}\text{K}_x\text{Fe}_2\text{As}_2$ ($\text{A}=\text{Ba}, \text{Sr}, \text{Ca}$, and Eu),⁶⁻⁹ Li_xFeAs ,¹⁰⁻¹² and FeSe_{1-x} (Ref. 13) are reported with their maximum T_C at about 38, 18, and 8 K, respectively.

The common features of the above mentioned FeAs-based superconductive compounds are that their phases adopt quasi-two-dimensional crystal structures in which superconducting [FeAs] layers are separated by either [LnO], [AO] layers or Li atomic sheets (except FeSe_{1-x}), which act as “charge reservoir.” Although the origin of superconductivity is unknown, it was recognized that (i) the undoped parent compounds LnFeAsO and AFe_2As_2 are located at the border of magnetic instability and exhibit temperature-dependent structure and magnetic phase transition with the formation of stripe antiferromagnetic; (ii) the bands around Fermi level are mainly derived from $[\text{Fe}_2\text{As}_2]$ block and in the range from -2 to $+2$ eV the DOS are mostly derived from Fe $3d$ state; and (iii) superconductivity appears with the doping (electron or hole) or under pressure, accompanying with the spin-density-wave (SDW) suppression.

Inspired by the results in LnFeAsO , Rotter⁶ predicted BaFe_2As_2 to be the parent compound of superconductor. After that, CaFe_2As_2 ,¹⁴ SrFe_2As_2 ,¹⁵ and EuFe_2As_2 (Ref. 16) are suggested to be the parent compounds of superconductor. In light of the experience in CuO-based superconductor, at the first stage, researchers changed the charge reservoir to look for new superconductor. They substituted A by alkali and found the superconductivity in $\text{A}_{1-x}\text{B}_x\text{Fe}_2\text{As}_2$ ($\text{B}=\text{Na}, \text{K}, \text{Rb}$, and Cs).^{17,18} Sooner, they focused on the [FeAs] layers because the bands around Fermi level are mainly derived from $[\text{Fe}_2\text{As}_2]$ block. Later, superconductivity were found in $\text{Ba}(\text{Fe}, \text{Ni}, \text{Co})_2\text{As}_2$.¹⁹ Recently, superconductivity in Ru substituted $\text{Sr}(\text{Ba})\text{Fe}_{2-x}\text{Ru}_x\text{As}_2$ was studied by experiment²⁰⁻²³ and theory calculation.^{24,25} This indicates that the supercon-

ductivity can be induced by substituting Fe with not only the $3d$ -transition metals, such as Co and Ni, but also with the $4d$ - and $5d$ -transition metals, such as Ru, Rh, Ir, and Pd.²⁰⁻²³ Transition elements in the $4d$ and $5d$ rows differ from their $3d$ counterparts in several respects. First, since $4d$ and $5d$ orbitals are much more extended than the $3d$ orbitals, there is a greater tendency toward covalency both with ligands As and also in stronger metal-metal d bonds. So, substitution $4d$ or $5d$ elements for Fe in FeAs compounds will enhance the hybridization with As and expand the bands around Fermi level, which will modify the properties of the compounds greatly. Second, again because of the more extended $4d$ and $5d$ orbitals, the Hund's coupling on these atoms is weaker than on $3d$ atoms, which works against magnetism since the Stoner parameter of Ru $I^{\text{Ru}}=0.6$ is smaller than that of Fe $I^{\text{Fe}}=0.9$.²⁶

In this paper, we reported first principles calculation results on $\text{SrFe}_{2-x}\text{Ru}_x\text{As}_2$. We found the isoelectronic substitution of Fe by Ru suppresses the spin-density-wave characteristic of SrFe_2As_2 by decreasing the Stoner enhancement and increasing the bandwidth due to the more extended Ru $4d$ band as compared with that of Fe $3d$. Although Ru is isoelectronic with Fe, such substitution changes the band structure and Fermi surface (FS). The phase diagram of $\text{SrFe}_{2-x}\text{Ru}_x\text{As}_2$ can be sorted as three different regions: (I) the stripe antiferromagnetic state ($0.0 \leq x < 0.6$); (II) the low spin state ($0.6 \leq x < 1.0$); and (III) the nonmagnetic state ($1.0 \leq x \leq 2.0$).

II. METHOD AND DETAILS

The calculations were done with the BSTATE (Ref. 27) code, with the ultrasoft pseudopotential plane-wave method. The nonmagnetic (NM) state, checkerboard antiferromagnetic (AF1) state, and the stripe antiferromagnetic (AF2) state were considered in this paper. All the lattice constants and the atomic positions were adopted from the x-ray diffraction data.²⁰ In order to study all the doping level, we used the virtual-crystal approximation (VCA) established by Bellaiche and Vanderbilt.²⁸ Here, we do not directly mix the pseudopotentials of Fe and Ru to make a new “artificial”

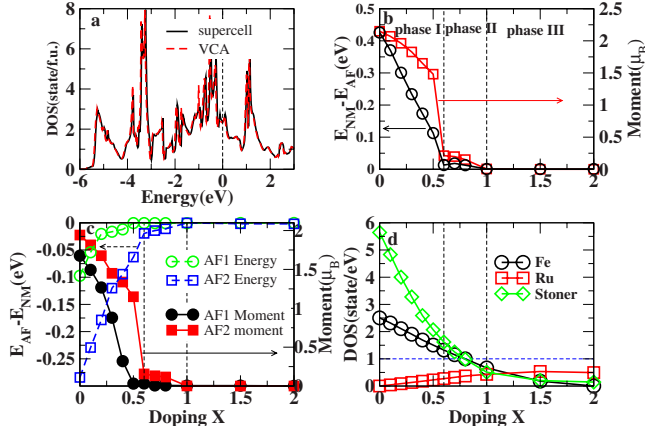


FIG. 1. (Color online) (a) A comparison of calculated DOS for SrFe_{1.5}Ru_{0.5}As₂. The solid curve is result obtained by supercell while the dashed curve gives the result by the VCA calculation. (b) With GGA approximation, the stabilization energy (per f.u.) and the moment of Fe atom, varying with Ru concentration. (c) With LDA approximation, the stabilization energy (per f.u.) and the moment of Fe atom, varying with Ru concentration. (d) The DOS at Fermi level of Fe [$N^{Fe}(E_F)$] and Ru [$N^{Ru}(E_F)$], the Stoner factor (defined in the text), varying with Ru concentration.

potential, just like the coherent-potential approximation.²⁹ On the contrary, we take Fe and Ru atoms to share the same lattice sites with different weights W_a . We have $W_{Fe} + W_{Ru} = 1$, so the total external pseudopotential is expressed by $V_{ext} = \sum_a W_a * V_{ps}^a$. With this VCA method, the partial density of states (PDOS) of Ru and Fe with different weights W_a can be well defined. After carefully checking the convergence with respect to the cut-off energy and the number of k points, we adopted a cut-off energy of 30 Ry for all the states and generated k points using the Monkhorst-Pack scheme with $10 \times 10 \times 16$ grids for the NM state and AF1 state with $8 \times 10 \times 10$ grids for the AF2 state.

III. RESULTS AND DISCUSSION

First, we test the reliability of substitution of Fe by Ru within the VCA for SrFe_{1.5}Ru_{0.5}As₂. Comparing the DOS obtained from the supercell and VCA calculation [see Fig. 1(a)], we find this VCA method is reliable for the present compound. Figure 1(b) shows the magnetic moment and stabilization energy of AF2 with generalized gradient approximation (GGA) calculation while Fig. 1(c) shows those of AF1 and AF2 with local-density approximation (LDA) calculation. In Fig. 1(c), we can see the ground state of SrFe_{2-x}Ru_xAs₂ is AF2 in the doping range from $x=0.0$ to 1.0. So we will mainly study the properties of AF2 and NM states in this paper. Comparing Figs. 1(b) and 1(c), we find that both the stabilization energy and magnetic moment are smaller within LDA than those of GGA, which is consistent with previous results on BaFe₂As₂ and LaOFeAs because GGA overestimates the magnetization in Fe-based compounds. However, GGA and LDA give the same tendency that the magnetization is suppressed with the Ru substitution. In Figs. 1(b)–1(d), the phase diagram of SrFe_{2-x}Ru_xAs₂ can

be sorted as three different phases: (I) the stripe antiferromagnetic state ($0.0 \leq x < 0.6$); (II) the low spin state ($0.6 \leq x < 1.0$); and (III) the nonmagnetic state ($1.0 \leq x \leq 2.0$). Because at the Fermi level the DOS is mainly derived from the Fe and Ru atoms, we defined the Stoner factor³⁰ of the compound as $I^{Fe} \times [N^{Fe}(E_F)]^2 + I^{Ru} \times [N^{Ru}(E_F)]^2$, where $N^{Fe}(E_F)$ and $N^{Ru}(E_F)$ are the density of states (at the Fermi level) of Fe and Ru, respectively. Here, $I^{Fe}(0.9)$ and $I^{Ru}(0.6)$ are the Stoner parameters of Fe and Ru.^{26,30} The stabilization energy, moment of Fe atom, $N^{Fe}(E_F)$, $N^{Ru}(E_F)$, and the Stoner factor vary with Ru substitution. We will study the properties of different phases in the following sections.

A. Phase I: the stripe antiferromagnetic state ($0.0 \leq x < 0.6$)

In this phase, SrFe_{2-x}Ru_xAs₂ almost preserves its property as SrFe₂As₂. In Figs. 1(b) and 1(c), the stabilization energy and the moment of Fe decrease rapidly with Ru substitution. At the same time, $N^{Fe}(E_F)$ decreases quickly, accompanying with $N^{Ru}(E_F)$ increasing. Let us first focus on the parent compound SrFe₂As₂ because its property is important to understand the substituted compounds. From the total density of states at the Fermi level for both spin channels $N(E_F)$, we can estimate the value of electron heat capacity γ (in mJ K⁻²) and the molar Pauli susceptibility χ_P (in 10⁻⁵ emu/mol) in the following relation: $\gamma = \frac{\pi^2}{3} k_B N(E_F) (1 + \lambda_{ep})$ and $\chi_P = \mu_B^2 N(E_F)$, where λ_{ep} is the electron-phonon coupling constant. As a first approximation, we set $\lambda_{ep} = 0$. For $x=0.0$ compound, the $N(E_F)$ is 5.4, which gives the electron-heat capacity $\gamma = 12.83$ and the molar Pauli susceptibility $\chi = 17.96$. Our calculated electron-heat capacity is only about half of the experimental³¹ one ($\gamma = 33$), which means strong correlation on Fe atom in SrFe₂As₂. The band structure and FS of SrFe₂As₂ are presented in Figs. 2(a) and 3(a), where three holelike FS circled around Γ point and two electronlike FS circled around X point. By shifting the FS around Γ point to X point, i.e., by a vector $q = (\pi, \pi, 0)$, the holelike FS will largely overlap with the electronlike FS, suggesting significant nesting effect. The existence of strong nesting effect would suggest that certain kinds of ordering, such as charge density wave or SDW,^{32,33} may develop at low temperature in the undoped compound, just like LaOFeAs,^{32,33} which has been proved by the experiment.³² The calculated results showed that the AF2 state is favored by 0.212 eV as compared with the NM state and the moment of Fe atom is $2.15 \mu_B$. The stabilization energy of SrFe₂As₂ is larger than that of LaFeAsO (0.189 eV), which may due to the moment of Fe atom in the former ($2.15 \mu_B$) is larger than in the latter ($1.7 \mu_B$).³³ Substituting Fe by Ru, the stabilization energy and the moment rapidly decrease to 0.06 eV and $0.21 \mu_B$, respectively. In this phase, the DOS of Fe and the Stoner factor quickly decrease with Ru substitution, accompanying with the increasing of DOS of Ru.

B. Phase II: the low spin state ($0.6 \leq x < 1.0$)

When the concentration of Ru is larger than $x=0.6$, the compounds enter into phase II: the low spin state, where the stabilization energy is smaller than 0.06 eV (per Fe atom)

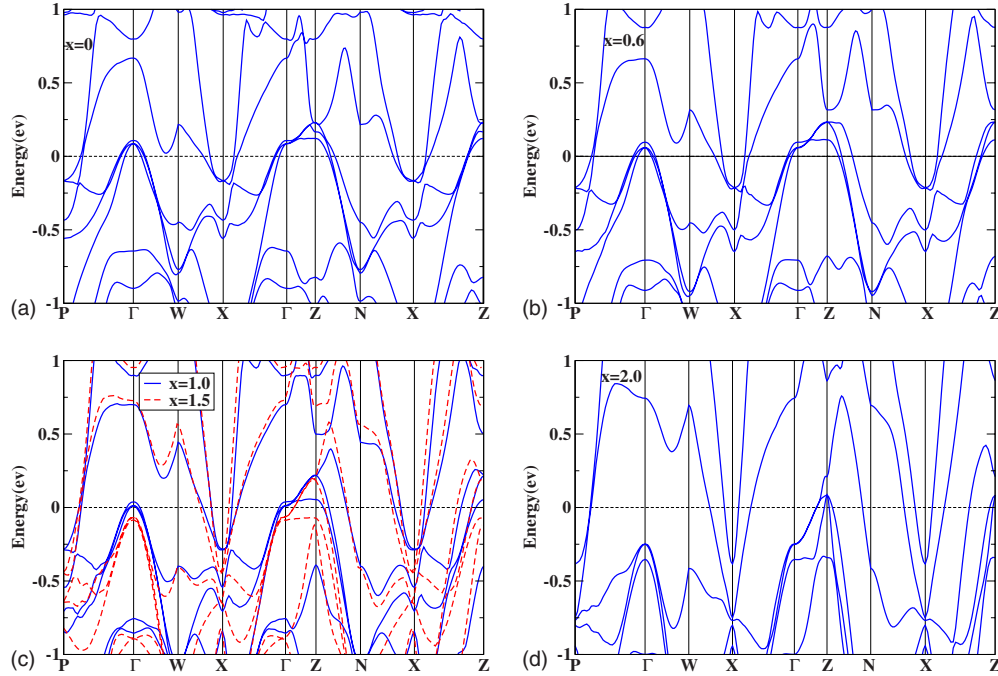


FIG. 2. (Color online) The band structure of SrFe_{2-x}Ru_xAs₂: (a) $x=0$, (b) $x=0.6$, (c) $x=1.0$ and $x=1.5$, and (d) $x=2.0$. In units of the tetragonal primitive reciprocal-lattice vectors, the special k points are denoted as $P(\frac{1}{2}, 0, \frac{1}{2})$, $\Gamma(0, 0, 0)$, $W(\frac{1}{4}, \frac{1}{4}, 0)$, $X(\frac{1}{2}, 0, 0)$, $Z(0, 0, \frac{1}{2})$, and $N(\frac{1}{4}, \frac{1}{4}, \frac{1}{2})$.

and the moment of Fe atom is smaller than $0.2\mu_B$. Such small moment is similar to that in LaOFeAs, where the experimental moment of Fe is $0.38\mu_B$. In this phase, the compounds are located at the border of magnetic instability, which will enhance the magnetic fluctuation.³⁴ Such magnetic fluctuation is believed to be important for the emergence of superconductivity.³⁴ From Fig. 1(d), it is clearly seen that the Stoner factor decreases with Ru substitution, which means that the Ru substitution reduces the DOS at the Fermi level and suppresses the magnetic instability induced by the Stoner mechanism. Such phenomena are similar to that of LaO_{1-x}F_xFeAs and Ba_{1-x}K_xFe₂As₂, where the elec-

tron and hole doping suppressed the SDW and the stripe antiferromagnetism. The superconductivity appears with the SDW suppression. Although the SDW is suppressed by Ru “doping,” such doping is significantly different with F atom doping in LaO_{1-x}F_xFeAs and K atom doping Ba_{1-x}K_xFe₂As₂. Because Ru is isoelectronic with Fe, substitution Fe by Ru introduces neither electron nor hole in the system.²⁴ The reason for the SDW suppressing is that the Ru 4d orbitals are much more extended than the Fe 3d orbitals, so the Hunds coupling on Ru atoms is weaker than on Fe atoms, which works against magnetism.

Comparing the band structure and FS of $x=0.6$ [Figs. 2(b) and 3(b)] with that of $x=0.0$ [Figs. 2(a) and 3(a)] we find that the bands and FS are hardly modified at X point while along Γ -Z line the FS show obviously three-dimensional character: shrinking at Γ point and expanding at Z point for $x=0.6$. For the $x=1.0$, such effect is further enhanced [see Figs. 2(c) and 3(c)]. In this phase superconductivity appears so it implies that the electrons on the FS along Γ -Z line may play important roles for the emergence of superconductivity. As mentioned above, both the stabilization energy and the moment are too small to stabilize the compound in the stripe antiferromagnetic state so the magnetic fluctuation greatly enhanced in this phase. Such magnetic fluctuation is believed to play important role for the emergence of superconductivity.³⁴ Therefore, the study of this doping range ($0.6 \leq x < 1.0$) would be important to seek new superconductor. Actually, Schnelle *et al.*²⁰ had found superconductivity in SrFe_{2-x}Ru_xAs₂ at $x=0.6, 0.7,$ and 0.8 , and Paulraj *et al.*²¹ reported superconductivity in BaFe_{2-x}Ru_xAs₂ with $T_c = 20.8$ K at $x=0.75$.

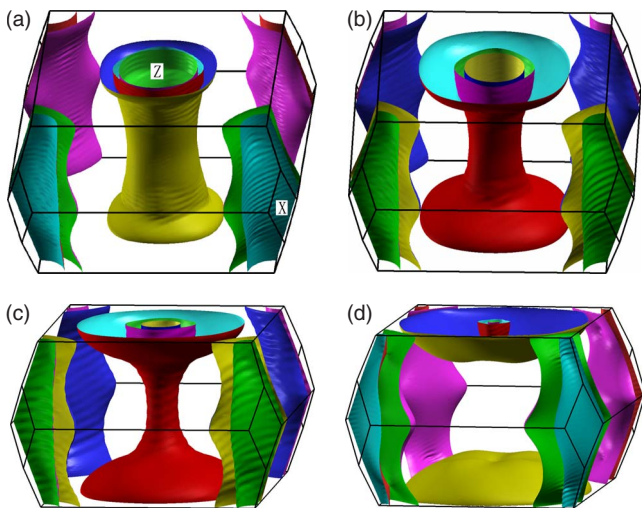


FIG. 3. (Color online) The Fermi surfaces of SrFe_{2-x}Ru_xAs₂: (a) $x=0$, (b) $x=0.6$, (c) $x=1.0$, and (d) $x=2.0$.

C. Phase III: the nonmagnetic state ($1.0 \leq x \leq 2.0$)

When $x > 1.0$ the compounds enter into the nonmagnetic state, where the compounds almost show the properties of SrRu_2As_2 . In Figs. 1(b) and 1(c), both the stabilization energy and the moment of Fe decrease to zero. At the same time, the Stoner factor decreases almost to zero. Therefore, the ground state of these compounds is nonmagnetic state in this phase. From the density of state at the Fermi energy for both spin channels $N(E_F) = 3.4$ (state/eV f.u.), we estimate the electron-heat capacity $\gamma = 3.9$ (in mJ K^{-2}) and the molar Pauli susceptibility $\chi = 5.5$ (in 10^{-5} emu/mol). Such results are perfect agree with Nath *et al.*'s³⁵ experimental values. In Fig. 2(c), the bands structure of $x = 1.5$ is significantly different with those of $x = 1.0$. For $x = 1.0$, there are three bands cut across the Fermi level at Γ point (blue and solid line) while for $x = 1.5$ (red and dashed line) these bands are suppressed below Fermi level. Therefore, when $x > 1.0$ the holelike Fermi surfaces along Γ -Z line disappeared [Fig. 3(d)], accompanying with the disappearance of superconductivity. Such results further imply that the FS along Γ -Z line and the magnetic fluctuation may play important roles for the emergence of superconductivity.

IV. SUMMARY AND CONCLUSION

In summary, by our first-principles calculations, the phase diagram of $\text{SrFe}_{2-x}\text{Ru}_x\text{As}_2$ can be sorted as three different

phases: (I) the stripe antiferromagnetic state ($0.0 \leq x < 0.6$); (II) the low spine state ($0.6 \leq x < 1.0$); and (III) the nonmagnetic state ($1.0 \leq x \leq 2.0$). Although Ru is isoelectronic with Fe, the stabilization energy and moment decrease rapidly with Ru substitution in Phase I. It is well known that the Ru $4d$ orbitals are more extended than the Fe $3d$ orbitals. Therefore, the Hund's coupling is weaker on Ru than on Fe atoms, which works against magnetism since the Stoner parameter I of Ru $I^{\text{Ru}} = 0.6$ is smaller than that of Fe $I^{\text{Fe}} = 0.9$. In phase II, both the stabilization energy and the moment are very small, so the magnetic fluctuation is greatly enhanced. Such magnetic fluctuation is believed to play important roles for the emergence of superconductivity. In phase III, the holelike Fermi surfaces along Γ -Z line and the magnetic fluctuation disappear, accompanying with the disappearance of superconductivity. Such results imply that the electrons on the FS along Γ -Z line and the magnetic fluctuation may play important roles for the emergence of superconductivity.

ACKNOWLEDGMENTS

The authors acknowledge the supports from NSF of China (Grants No. No.10947001 and No. 10674042)

-
- ¹Y. Kamihara, T. Watanabe, M. Hirano, and H. Hosono, *J. Am. Chem. Soc.* **130**, 3296 (2008).
- ²X. H. Chen, T. Wu, G. Wu, R. H. Liu, H. Chen, and D. F. Fang, *Nature (London)* **453**, 761 (2008).
- ³G. F. Chen, Z. Li, D. Wu, G. Li, W. Z. Hu, J. Dong, P. Zheng, J. L. Luo, and N. L. Wang, *Phys. Rev. Lett.* **100**, 247002 (2008).
- ⁴Z. A. Ren, J. Yang, W. Lu, W. Yi, X. L. Shen, Z. C. Li, G. C. Che, X.-L. Dong, L. L. Sun, F. Zhou, and Z. X. Zhao, *EPL* **82**, 57002 (2008).
- ⁵Z. A. Ren, L. Wei, Y. Jie, Y. Wei, S. X. Li, Z. Cai, C. G. Can, D. X. Li, S. L. Ling, Z. Fang, and Z. Z. Xian, *Chin. Phys. Lett.* **25**, 2215 (2008).
- ⁶M. Rotter, M. Tegel, D. Johrendt, I. Schellenberg, W. Hermes, and R. Pöttgen, *Phys. Rev. B* **78**, 020503(R) (2008).
- ⁷M. Rotter, M. Tegel, and D. Johrendt, *Phys. Rev. Lett.* **101**, 107006 (2008).
- ⁸K. Sasmal, B. Lv, B. Lorenz, A. M. Guloy, F. Chen, Y. Y. Xue, and C. W. Chu, *Phys. Rev. Lett.* **101**, 107007 (2008).
- ⁹H. Ding, P. Richard, K. Nakayama, K. Sugawara, T. Arakane, Y. Sekiba, A. Takayama, S. Souma, T. Sato, T. Takahashi, Z. Wang, X. Dai, Z. Fang, G. F. Chen, J. L. Luo, and N. L. Wang, *EPL* **83**, 47001 (2008).
- ¹⁰G. Wu, R. H. Liu, H. Chen, Y. J. Yan, T. Wu, Y. L. Xie, J. J. Ying, X. F. Wang, D. F. Fang, and X. H. Chen, *EPL* **84**, 27010 (2008).
- ¹¹J. H. Tapp, Z. J. Tang, B. Lv, K. Sasmal, B. Lorenz, Paul C. W. Chu, and A. M. Guloy, *Phys. Rev. B* **78**, 060505(R) (2008).
- ¹²X. C. Wang, Q. Q. Liu, Y. X. Lv, W. B. Gao, L. X. Yang, R. C. Yu, F. Y. Li, and C. Q. Jin, *Solid State Commun.* **148**, 538 (2008).
- ¹³F. C. Hsu, J. Y. Luo, K. W. Yeh, T. K. Chen, T. W. Huang, P. M. Wu, Y. C. Lee, Y. L. Huang, Y. Y. Chu, D. C. Yan, and M. K. Wu, *Proc. Natl. Acad. Sci. U.S.A.* **105**, 14262 (2008).
- ¹⁴Jun Zhao, D. T. Adroja, Dao-Xin Yao, R. Bewley, Shiliang Li, X. F. Wang, G. Wu, X. H. Chen, Jiangping Hu, and Pengcheng Dai, *Nat. Phys.* **5**, 555 (2009).
- ¹⁵J. Zhao, W. Ratcliff, J. W. Lynn, G. F. Chen, J. L. Luo, N. L. Wang, J. Hu, and P. Dai, *Phys. Rev. B* **78**, 140504(R) (2008).
- ¹⁶Z. Ren, Z. Zhu, S. Jiang, X. Xu, Q. Tao, C. Wang, C. Feng, G. Cao, and Z. A. Xu, *Phys. Rev. B* **78**, 052501 (2008).
- ¹⁷L. Wray, D. Qian, D. Hsieh, Y. Xia, L. Li, J. G. Checkelsky, A. Pasupathy, K. K. Gomes, C. V. Parker, A. V. Fedorov, G. F. Chen, J. L. Luo, A. Yazdani, N. P. Ong, N. L. Wang, and M. Z. Hasan, *Phys. Rev. B* **78**, 184508 (2008).
- ¹⁸A. A. Aczel, E. Baggio-Saitovitch, S. L. Budko, P. C. Canfield, J. P. Carlo, G. F. Chen, Pengcheng Dai, T. Goko, W. Z. Hu, G. M. Luke, J. L. Luo, N. Ni, D. R. Sanchez-Candela, F. F. Tafti, N. L. Wang, T. J. Williams, W. Yu, and Y. J. Uemura, *Phys. Rev. B* **78**, 214503 (2008).
- ¹⁹M. A. Tanatar, N. Ni, C. Martin, R. T. Gordon, H. Kim, V. G. Kogan, G. D. Samolyuk, S. L. Budko, P. C. Canfield, and R. Prozorov, *Phys. Rev. B* **79**, 094507 (2009); A. S. Sefat, M. A. McGuire, R. Jin, B. C. Sales, D. Mandrus, F. Ronning, E. D. Bauer, and Y. Mozharivskiy, *ibid.* **79**, 094508 (2009); M. S. da Luz, J. J. Neumeier, R. K. Bollinger, A. S. Sefat, M. A. McGuire, R. Jin, B. C. Sales, and D. Mandrus, *ibid.* **79**, 214505 (2009).
- ²⁰W. Schnelle, A. Leithe-Jasper, R. Gumeniuk, U. Burkhardt, D.

- Kasinathan, and H. Rosner, Phys. Rev. B **79**, 214516 (2009).
- ²¹S. Paulraj, S. Sharma, A. Bharathi, A. T. Satya, S. Chandra, Y. Hariharan, and C. S. Sundar, arXiv:0902.2728 (unpublished).
- ²²Y. Qi, L. Wang, Z. Gao, D. Wang, X. Zhang, and Y. Ma, arXiv:0903.4967 (unpublished).
- ²³F. Han, X. Zhu, P. Cheng, G. Mu, Y. Jia, L. Fang, Y. Wang, H. Luo, B. Zeng, B. Shen, L. Shan, C. Ren, and H.-H. Wen, Phys. Rev. B **80**, 024506 (2009).
- ²⁴L. Zhang and D. J. Singh, Phys. Rev. B **79**, 174530 (2009).
- ²⁵I. R. Shein and A. L. Ivanovskii, arXiv:0905.2255 (unpublished).
- ²⁶O. K. Andersen, J. Madsen, U. K. Poulsen, O. Jepsen, and J. Kollar, Physica C **86-88**, 249 (1977); E. C. Stoner, Proc. R. Soc. London, Ser. A **165**, 372 (1938).
- ²⁷Z. Fang and K. Terakura, J. Phys.: Condens. Matter **14**, 3001 (2002).
- ²⁸L. Bellaiche and David Vanderbilt, Phys. Rev. B **61**, 7877 (2000).
- ²⁹P. Soven, Phys. Rev. **156**, 809 (1967).
- ³⁰I. I. Mazin and D. J. Singh, Phys. Rev. B **56**, 2556 (1997).
- ³¹J. Q. Yan, A. Kreyssig, S. Nandi, N. Ni, S. L. Budko, A. Kracher, R. J. McQueeney, R. W. McCallum, T. A. Lograsso, A. I. Goldman, and P. C. Canfield, Phys. Rev. B **78**, 024516 (2008).
- ³²J. Dong, H. J. Zhang, G. Xu, Z. Li, G. Li, W. Z. Hu, D. Wu, G. F. Chen, X. Dai, J. L. Luo, Z. Fang, and N. L. Wang, EPL **83**, 27006 (2008); C. de la Cruz, Q. Huang, J. W. Lynn, Jiying Li, W. Ratcliff II, J. L. Zarestky, H. A. Mook, G. F. Chen, J. L. Luo, N. L. Wang, and Pengcheng Dai, Nature (London) **453**, 899 (2008).
- ³³D. J. Singh and M. H. Du, Phys. Rev. Lett. **100**, 237003 (2008); G. Xu, W. Ming, Y. Yao, X. Dai, S.-C. Zhang, and Z. Fang, EPL **82**, 67002 (2008).
- ³⁴A. J. Drew, F. L. Pratt, T. Lancaster, S. J. Blundell, P. J. Baker, R. H. Liu, G. Wu, X. H. Chen, I. Watanabe, V. K. Malik, A. Dubroka, K. W. Kim, M. Rössle, and C. Bernhard, Phys. Rev. Lett. **101**, 097010 (2008); R. H. Liu, *et al.*, *ibid.* **101**, 087001 (2008); M. M. Korshunov and I. Eremin, Phys. Rev. B **78**, 140509(R) (2008); H. H. Klauss, *et al.*, Phys. Rev. Lett. **101**, 077005 (2008); F. Bondino, *et al.*, *ibid.* **101**, 267001 (2008).
- ³⁵R. Nath, Yogesh Singh, and D. C. Johnston, Phys. Rev. B **79**, 174513 (2009).